The Modification of Fly Ash with Regional Clay in Thailand for Alternative Ceramic Product

Prapatsorn Prathungthai

Department of Ceramics Design, Faculty of Architecture and Design,

King Mongkut's University of Technology North Bangkok, Thailand

Abstract

This research aims to study the modification of fly ash mixed with Dan Kwian clay, dolomite, feldspar, and kaolin for ceramic production. A triaxial blend model was chosen to design raw material content. Firing shrinkage, water absorption, and Rockwell hardness were applied for the specimen test. The incompatibility of mixed raw material illustrated the cracking, breaking, and deformation including the melting of specimens after the firing process. The tendency of firing shrinkage increases whereas water absorption decreases at higher temperatures. The reasonable mixed raw material obtaining dolomite, Dan Kwian clay, and fly ash of 60 wt%, 20 wt%, and 20 wt%, respectively, calcined at 1,200 ˚C served the stable firing shrinkage, relatively low water absorption, and the highest Rockwell hardness. The product of the ceramic plant pot fabricated as the preliminary test with the recommended condition demonstrated a satisfying smooth surface, strength, and shininess.

Keywords*:* Fly ash, Dan Kwian clay, Triaxial blend model, Firing shrinkage, Water absorption, Rockwell hardness

1. Introduction

Throughout the world, much research is being proceeded on the benefit of waste products to either avoid an expanding toxic threat to the environment or to streamline present waste handling techniques by making them rather affordable [1]. Since broad-scale coal firing for power generation began in the 1920s, abundant millions of tons of ash and related by-products have been generated [2,3]. The quantity of fly ash (coal waste), released by manufacturing and thermal power plants has been increasing throughout the world, and the displacement of a large amount of fly ash (waste material) has become a serious environmental problem [2,3]. Meantime, the present annual production of coal ash worldwide is estimated at 600 million tonnes, with fly ash constituting around 500 million tonnes at 75-80% of the total ash produced [4]. A considerable quantity of ash is still ridden in landfills and/or lagoons at a significant cost to the utilizing companies and thus to the consumers, while the world utilization of ash is only 16% of the total ash [2]. Nowadays, finding means of utilizing fly ash is an extremely important field of research. In Thailand, Mae Moh coal-fired power plant (Lampang province, Thailand) mostly generated lignite fly ash [5], which is output between 3.0 to 3.5 million tons of fly ash per year and 1.5 to 2.0 million tons of bottom ash per year [6]. Fly ash is known to be used to replace Portland cement to decrease production costs and increase product properties, but it is not very helpful. Notwithstanding, normal chemical compositions of fly ash contain quartz

(Si_2O_3), anorthite ($CaAl_2Si_2O_8$), hematite (Fe_2O_3), etc., which are similar to raw materials of ceramic tile [7]. At the same time, the ceramics industry employs clay in the manufacture of bricks, generic ceramics, glass, heavy clay products, aggregates, tiles, and refractory products [8]. Dan Kwian clay is one famous clay for the household ceramic industry at Nakhon Ratchasima (Thailand) because it is simple to fabricate, and firing resistant, providing unique beauty derived from the nature of iron or iron rust in Dan Kwian clay [9].

In this work, the study of fly ash mixing with Dan Kwian clay, dolomite, feldspar, and kaolin is presented. Three factors containing three raw materials were designed through the triaxial blend model. Firing shrinkage, water absorption, and Rockwell hardness were chosen to test the physical property of specimens. The chemical compositions in the best composition condition were analyzed and offered to fabricate the ceramic plant pot as a prelim product ahead of recommending it to the ceramic industry.

2. Raw materials and methods

The raw materials with the chemical contents used in this work were inferior dolomite ($CaMg(CO_3)_2$), feldspar ($KAlSi_3O_8$- $NaAlSi_3O_8$- $CaAl_2Si_2O_8$) [10], kaolin ($Al_2Si_2O_5(OH)_4$), Dan Kwian clay (75wt%SiO_2-16wt%Al_2O_3-5wt%Fe_2O_3-1wt%K_2O) [11], and fly ash (41wt%SiO_2-20wt%Al_2O_3-14wt%Fe_2O_3-11wt%CaO-6wt%MgO-4wt%Na_2O-other chemicals) [12]. Dan Kwian clay was provided by Mitdinpow Ceramic, Dan Kwian subdistrict, Chok Chai District, Nakhon Ratchasima (Thailand). Fly ash was supplied by Mae Moh coal-fired power plant, Mae Moh district, Lampang (Thailand). Dolomite, feldspar, kaolin, and clear glaze in the technical grade were bought by Compound Clay Co. Ltd.

The weight percentage of specimens is divided into 3 factors using a triaxial blend model as demonstrated in Figure 1 (Factor 1 including dolomite, Dan Kwian clay, and fly ash, factor 2 consisting of feldspar, Dan Kwian clay, and fly ash, and factor 3 comprising kaolin, Dan Kwian clay, and fly ash. The preparation process is shown in Figure 2. Dan Kwian clay was dried under sunlight for about 8 h and crushed to powder. The crushed Dan Kwian clay was soaked in water overnight and then stirred until the solution becomes homogenous, the aging process proceeded for 12 h. The prepared Dan Kwian clay powder was blended with feldspar, kaolin, or fly ash employing suitable water according to each factor and a triaxial blend. The blended materials were homogeneously stirred. Thirty-six specimens for each factor were formed using the plaster molding with a width of 2 mm, length of 12 mm, and height of 1.5 cm. Specimens were calcined at 800 °C and 1,200 °C (each temperature consisting of 108 specimens from 3 factors) for 6 h with a heating rat at 5 °C/min.

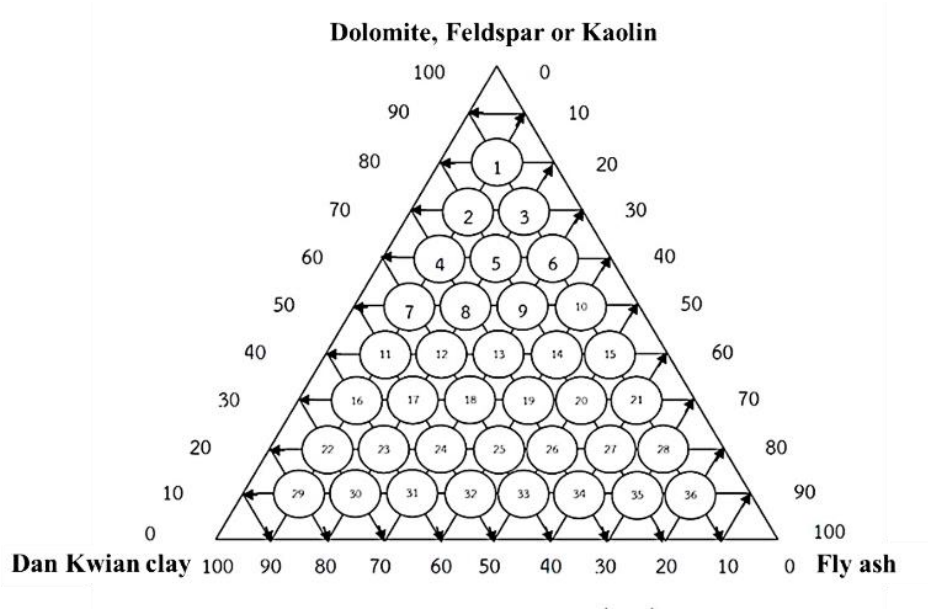

Figure 1 Triaxial graph representing the weight percent of the solution composition with different factors.

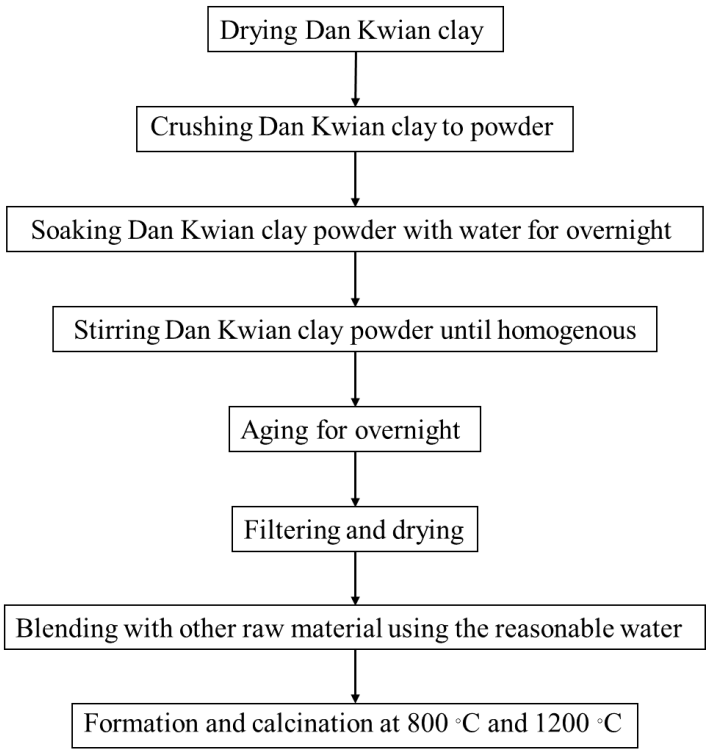

Figure 2 Preparation of Dan Kwian clay for blending with other raw materials.

After calcination, the remained specimens (without deformation, melting, or broken to powder during the calcination procedure) were then tested to obtain the firing technological properties related to the firing shrinkage, water absorption, and Rockwell hardness. The firing shrinkage (ASTM C 326) was obtained by the length of the samples before (L_B) and after (L_A) the calcine stage and were calculated with equation (1).

$$\text{Firing shrinkage (\%)} = \frac{L_B - L_A}{L_B} \quad (1)$$

The water absorption was calculated for each specimen, using the formula in Equation (2), according to ISO 10545-3.

$$\text{Water absorption (\%)} = \frac{W_2 - W_1}{W_1} \quad (2)$$

Where W_1 is the weight of the dry specimen, W_2 is the weight of the wet specimen.
Rockwell hardness measurement was performed with an HR-150A (Laizhou Exp., Shandong, China), and this was carried out under ASTM E18 standard test method. The chemical compositions of the promising condition were obtained using an energy-dispersive X-ray fluorescence (EDXRF; EDAX Smart Insight, ORBIS PC, NJ, USA). The selected composition condition was molded to be the ceramic plant pot via wheel throwing.

3. Results and discussions

According to the calcination of specimens before physical tests, most specimens cracked or broken to powder during the firing process, especially at 800 ˚C. This result may be due to the inappropriate raw material composition. The deformation or melting of specimens mostly occurs at 1,200 ˚C because some raw material (feldspar) can reduce the transformation temperature resulting in the deformation of specimens at a low temperature [13]. The percentage of firing shrinkage with the different factors calcined at 800˚C is listed in Table 1. As seen in Table 1, factors 1 and 2 demonstrated the firing shrinkage lower than that of factor 3. The higher firing shrinkage was remarked in factor 3 due to the dehydroxylation process of the kaolin. [14]. However, the negative percent firing shrinkage shown with some specimens owing to the enlargement of mixed material during to calcination process, and the phase transformation of the different chemical compositions [15]. The zero percent firing shrinkage can be observed in specimens no. 5, 7, 8, 11, 12, 13, and 14 for factor 1 and specimens no. 12 and 13 for factor 2. These results suggested that the raw material content provides compatibility with their chemical composition.

Table 1 The percentage of firing shrinkage with the different factors calcined at 800˚C

No.	Firing shrinkage (%) at 800 ˚C			No.	Firing shrinkage (%) at 800 ˚C		
	Factor 1	Factor 2	Factor 3		Factor 1	Factor 2	Factor 3
1	1	-10	3	19	1	1	3
2	n.d.*	-7	3	20	n.d.*	1	3
3	n.d.*	-9	3	21	n.d.*	n.d.*	3
4	1	-6	3	22	1	2	3
5	0	-2	3	23	1	2	3
6	n.d.*	1	3	24	3	1	3
7	0	1	4	25	1	1	4
8	0	1	3	26	1	1	3
9	n.d.*	1	3	27	n.d.*	n.d.*	3
10	n.d.*	1	3	28	n.d.*	n.d.*	3

11	0	1	5	29	2	2	5
12	0	0	3	30	2	1	3
13	0	0	3	31	1	2	3
14	0	1	5	32	1	1	5
15	n.d.*	n.d.*.	3	33	1	2	3
16	1	1	4	34	1	n.d.*	4
17	2	2	3	35	-1	n.d.*	3
18	2	1	3	36	-2	n.d.*	3

n.d.* (Not detected): specimens are cracked or become powder during the calcination procedure.

Table 2 presents the compositions of specimens in terms of the different factors and the measured values for firing shrinkage at 1,200 ˚C. As illustrated in Table 2, only factors 1 and 3 provided the firing shrinkage data, whereas all specimens in factor 2 are melted or deformed. The mixed feldspar in the composition of specimens caused the melting of specimens in factor 2 because the chemical composition of feldspar acts as a sintering aid promoting the firing process at a lower temperature [16]. The higher firing shrinkage can observe in factor 3 while some specimens disclose the lower and negative firing shrinkage (the explanation as above mentioned). Nevertheless, specimens no. 5, 7, and 13 in factor 1 remained a zero firing shrinkage compared to the calcination at 800 ˚C.

Table 2 The percentage of firing shrinkage with the different factors calcined at 1,200 ˚C

No.	Firing shrinkage (%) at 1,200 ˚C			No.	Firing shrinkage (%) at 1,200 ˚C		
	Factor 1	Factor 2	Factor 3		Factor 1	Factor 2	Factor 3
1	2	n.d.**	9	19	-1	n.d.**	7
2	0	n.d.**	9	20	-2	n.d.**	7
3	-1	n.d.**	9	21	-4	n.d.**	7
4	-2	n.d.**	9	22	n.d.**	n.d.**	7
5	0	n.d.**	7	23	n.d.**	n.d.**	n.d.**
6	-5	n.d.**	8	24	n.d.**	n.d.**	8
7	0	n.d.**	9	25	8	n.d.**	10
8	-1	n.d.**	7	26	3	n.d.**	9
9	-2	n.d.**	6	27	n.d.**	n.d.**	8
10	n.d.**	n.d.**	6	28	n.d.**	n.d.**	5
11	3	n.d.**	10	29	n.d.**	n.d.**	9
12	2	n.d.**	10	30	n.d.**	n.d.**	11
13	0	n.d.**	6	31	n.d.**	n.d.**	n.d.**
14	-1	n.d.**	6	32	n.d.**	n.d.**	n.d.**
15	n.d.**	n.d.**	8	33	n.d.**	n.d.**	n.d.**
16	5	n.d.**	8	34	n.d.**	n.d.**	n.d.**
17	4	n.d.**	8	35	n.d.**	n.d.**	n.d.**
18	1	n.d.**	7	36	n.d.**	n.d.**	n.d.**

n.d.**: specimens are deformed or melted during the calcination procedure.

Table 3 demonstrates the water absorption data fired at 800 ˚C. As can be seen, factors 1 and 3 revealed relatively higher average water absorption (20% of factor 1 and 21% of factor 3) whereas lower average water absorption (13%) obtaining in factor 2. This information indicates the porosity of raw materials such as SiO_2 and Al_2O_3 contained in factors 1 and 3 resulting in higher water absorption [17,18]. Moreover, the mixed dolomite is relatively highly absorbed in water [19]. Meantime, feldspar may accelerate the melting point causing the decrease of porosity in the raw material [20]. The lowest water absorption of each factor is No. 36 (10.1%), No. 13 (10.2%), and No. 34 (14.1%) for factors 1, 2, and 3, respectively.

Table 3 The percentage of water absorption with the different factors calcined at 800 ˚C

No.	Water absorption (%) at 800 ˚C			No.	Water absorption (%) at 800 ˚C		
	Factor 1	Factor 2	Factor 3		Factor 1	Factor 2	Factor 3
1	27.2	13.3	31.3	19	19	13	19.7
2	n.d.*	14.1	29.5	20	n.d.*	13.2	16.7
3	n.d. *	12.5	31.1	21	n.d.*	n.d.*	16
4	25.7	13.4	28.3	22	19	13.2	20.2
5	25	12.5	30.2	23	20.7	14.2	20.4
6	n.d.*	11.5	27.3	24	17.7	14.6	20.4
7	25.1	12.1	26.7	25	18	14	16.2
8	24.5	13.5	25.9	26	19.4	15.4	17.2
9	n.d.*	12.2	25.7	27	n.d.*	n.d.*	16.1
10	n.d.*	10.5	24.5	28	n.d.	n.d.*	15.7
11	25.3	10.9	22.8	29	16.4	14.5	17
12	23.9	10.2	25.5	30	16.8	14.5	16.4
13	20.9	10.2	26	31	16.5	13.47	17.1
14	20.6	13.4	21.1	32	16.6	n.d.*	15.6
15	n.d.*	n.d.*	22.5	33	15.2	14.2	14.8
16	19.4	12.7	20.8	34	15.8	n.d.*	14.1
17	21.1	12.9	22	35	16.4	n.d.*	14.3
18	13.9	13.9	19.5	36	10.1	n.d.*	15.4

n.d.*: specimens are cracked or become powder during the calcination.

Table 4 presents the water absorption with the different factors calcined at 1,200 ˚C. As shown, all specimens in factor 2 are deformed or melted during the firing process regarding the addition of the sintering aid as above mention. Meanwhile, the averaged water absorption of 18% and 12% is illustrated in factors 1 and 3, respectively. Compared to the calcination of 800 ˚C, the water absorption decreased on average by 2% (factor 1) and 9% (factor 3) because the phase transformation (the densification of the body promoting partial removal of porosity) led to a noticeable reduction in porosity of raw materials could occur at a relatively high calcination process [21]. The lowest water absorption of each factor is No. 5 (15%) and No. 26 (0.8%) for factors 1 and 3, respectively.

Table 4 The percent of water absorption with the different factors calcined at 1,200 ˚C

No.	Water absorption (%) at 1,200 ˚C			No.	Water absorption (%) at 1,200 ˚C		
	Factor 1	Factor 2	Factor 3		Factor 1	Factor 2	Factor 3
1	17.9	n.d.**	16.6	19	19.4	n.d.**	11.8
2	18.7	n.d.**	16.6	20	20.6	n.d.**	9.5
3	17.9	n.d.**	20.1	21	20.3	n.d.**	9.9
4	19.8	n.d.**	18.3	22	n.d.**	n.d.**	9
5	15	n.d.**	19.4	23	n.d.**	n.d.**	n.d.**
6	17.7	n.d.**	20.2	24	n.d.**	n.d.**	5.6
7	17.9	n.d.**	15.9	25	16.6	n.d.**	1
8	17.5	n.d.**	16.8	26	17.4	n.d.**	0.8
9	18.5	n.d.**	17.1	27	n.d.**	n.d.**	6.1
10	n.d.**	n.d.**	15.1	28	n.d.**	n.d.**	8.1
11	16.2	n.d.**	12.1	29	n.d.**	n.d.**	6.5
12	16.7	n.d.**	12.8	30	n.d.**	n.d.**	1.3
13	15.2	n.d.**	13.4	31	n.d.**	n.d.**	n.d.**
14	18	n.d.**	13.7	32	n.d.**	n.d.**	n.d.**
15	n.d.**	n.d.**	7.8	33	n.d.**	n.d.**	n.d.**
16	16	n.d.**	10.23	34	n.d.**	n.d.**	n.d.**
17	20.8	n.d.**	12.1	35	n.d.**	n.d.**	n.d.**
18	16.4	n.d.**	14.3	36	n.d.**	n.d.**	n.d.**

n.d.**: specimens are deformed or melted during the calcination.

Corresponding to interpretation in Table 4, the suitable raw material composition calcined at 800 ˚C can be recommended to factor 2 No. 12 with feldspar, Dan Kwian clay, and fly ash of 40 wt%, 40 wt%, and 20 wt%, respectively and No. 13 with feldspar, Dan Kwian clay, and fly ash of 40 wt%, 30 wt%, and 30 wt%, respectively owing to the zero firing shrinkage and low water absorption. At the calcination of 1,200 ˚C, the reasonable content for the ceramic production is factor 1 comprising No. 5 with dolomite, Dan Kwian clay, and fly ash of 60 wt%, 20 wt%, and 20 wt%, respectively, and No. 13 with dolomite, Dan Kwian clay, and fly ash of 40 wt%, 30 wt%, and 30 wt%, respectively because of the unchanged shape and relatively low water absorption. All reasonable specimens were measured hardness by the Rockwell C scale technique, which is listed in Table 5. As seen in Table, a similar result is presented for all specimens (≥120 HRC). Nonetheless, No. 5 in factor 1 calcined at 1,200 ˚C showed the highest hardness value (128 HRC).

Table 5 Rockwell hardness of the appropriate composition for each calcination temperature

Calcination of 800 ˚C (factor 2)		Calcination of 1,200 ˚C (factor 1)	
No. 12	122 HRC	No. 5	128 HRC
No. 13	120 HRC	No. 13	127 HRC

Regarding unchanged shape, relatively low water absorption and the highest hardness value for specimen No.5 at calcination of 1,200 ˚C (factor 1), the final chemical compositions are presented in Table 6. The main chemical compositions are CaO, SiO_2, Al_2O_3 and Fe_2O_3 which are relative to the chemical composition of raw materials.

Table 6 EDXRF analysis of specimen No.5 at calcination of 1,200 ˚C for factor 1

Chemical composition	SiO_2	Al_2O_3	K_2O	CaO	MnO	Fe_2O_3	ZnO	SrO
Content (%)	17.4	15.6	0.3	54.3	0.1	12.1	0.1	0.1

Thus, specimen No.5 in factor 1 with calcination of 1,200 ˚C was chosen to form the product of a ceramic plant pot as demonstrated in Figure 3. After forming the plant pot structure (Figure 3 (a)), the stable structure can be observed and provided a satisfying smooth surface and shininess after being coated with clear glaze along with the firing process (Figure 3 (b)).

Figure 3 Product of a ceramic plant pot using the raw material composition of No. 5 (calcined at 1,200 ˚C) with dolomite, Dan Kwian clay, and fly ash of 60 wt%, 20 wt%, and 20 wt%, respectively: (a) before and (b) after coating with clear glaze and firing process.

4. Conclusion

The fly ash mixed with Dan Kwian clay, dolomite, feldspar, and kaolin to produce ceramic was introductory studied. The triaxial blend model helped in finding the reasonable raw material content through three factors. Improper raw material composition caused cracking or breaking of specimens (calcined at 800 ˚C) and deformation or melting of specimens (calcined at 1,200 ˚C). The firing shrinkage tends to increase when calcined at a higher temperature whereas water absorption tends to be decreased. Specimens No. 5, 7, and 13 in factor 1 for both calcined at 800 ˚C and 1,200 ˚C provided zero percent firing shrinkage. Among all specimens, No. 36 in factor 3 (calcined at 1,200 ˚C) reached the lowest water absorption of 0.8%. In summary, the recommended raw material composition to produce ceramic is No.5 in factor 1 calcined at 1,200 ˚C with dolomite, Dan Kwian clay, and fly ash of 60 wt%, 20 wt%, and 20 wt%, respectively due to zero percent firing shrinkage, acceptable water absorption, and highest hardness. The product of the ceramic plant pot formed as the preliminary test showed a

satisfying smooth surface, strength, and shininess which could be applied in the ceramic industry.

Acknowledgments

This work was financially supported by the Science and Technology Research Institute, King Mongkut's University of Technology North Bangkok (Grant No. KMUTBN-GEN-59-61).

Conflicts of interest

The authors have no conflicts of interest to declare.

Author's Contribution Statement

Prapatsorn Prathungthai: Conceptualization, formal analysis, methodology, validation and writing draft.

References

[1] Van Jaarsveld JGS, Van Deventer JSJ, Lorenzen L. Factors affecting the immobilization of metals in geopolymerized flyash. Metall Mater Trans B Process Metall Mater Process Sci 1998;29:283–91. https://doi.org/10.1007/s11663-998-0032-z.

[2] Ahmaruzzaman M. A review on the utilization of fly ash. Prog Energy Combust Sci 2010;36:327–63. https://doi.org/10.1016/j.pecs.2009.11.003.

[3] Wang L, Sun H, Sun Z, Ma E. New technology and application of brick making with coal fly ash. J Mater Cycles Waste Manag 2016;18:763–70. https://doi.org/10.1007/s10163-015-0368-9.

[4] Rashad AM. A brief on high-volume Class F fly ash as cement replacement – A guide for Civil Engineer. Int J Sustain Built Environ 2015;4:278–306. https://doi.org/10.1016/j.ijsbe.2015.10.002.

[5] Yoriya S, Tepsri P. Separation process and microstructure-chemical composition relationship of cenospheres from lignite fly ash produced from coal-fired power plant in Thailand. Appl Sci 2020;10:1–21. https://doi.org/10.3390/app10165512.

[6] Prasartseree T, Wasanapiarnpong T, Mongkolkachit C, Jiraborvornpongsa N. Influence of lignite bottom ash on pyroplastic deformation of stoneware ceramic tiles. Key Eng Mater 2018;766 KEM:264–9. https://doi.org/10.4028/www.scientific.net/KEM.766.264.

[7] Anufrik SS, Kurian NN, Zhukova II, Znosko KF, Belkov M V. Chemical Composition of Ceramic Tile Glazes. J Appl Spectrosc 2016;83:764–70. https://doi.org/10.1007/s10812-016-0360-8.

[8] Fuchs Y. Clays, Economic Uses. Encycl. Geol., Elsevier Inc.; 2004, p. 366–70. https://doi.org/10.1016/B0-12-369396-9/00256-2.

[9] Duangkhachon K, Kamon-In O. The development of Dan-Kwian ceramic jewelry for contemporary aesthetics in Nakhon Ratchasima Province. Key Eng Mater 2018;766 KEM:44–50. https://doi.org/10.4028/www.scientific.net/KEM.766.44.

[10] Rattanakawin C, Thacom B. Froth flotation of mixed feldspar. Songklanakarin J Sci Technol 2019;41:1314–8.

[11] STEIN SJ, UGEL L. Effect of Firing Conditions on Stability and Properties of Glaze

Resistors 1968;21:189–209. https://doi.org/10.14456/sjst.2014.10.
[12] Torkittikul P, Chaipanich A. Utilization of ceramic waste as fine aggregate within Portland cement and fly ash concretes. Cem Concr Compos 2010;32:440–9. https://doi.org/10.1016/j.cemconcomp.2010.02.004.
[13] Carbajal L, Rubio-Marcos F, Bengochea MA, Fernandez JF. Properties related phase evolution in porcelain ceramics. J Eur Ceram Soc 2007;27:4065–9. https://doi.org/10.1016/j.jeurceramsoc.2007.02.096.
[14] Malee U, Thiansem S. Preparation and characterization of clays from different areas in Ban Bo Suak, Nan province, Thailand. Key Eng. Mater., vol. 659, Trans Tech Publications Ltd; 2015, p. 127–31. https://doi.org/10.4028/www.scientific.net/KEM.659.127.
[15] Baccour H, Medhioub M, Jamoussi F, Mhiri T. Influence of firing temperature on the ceramic properties of Triassic clays from Tunisia. J Mater Process Technol 2009;209:2812–7. https://doi.org/10.1016/j.jmatprotec.2008.06.055.
[16] Ma H, Tian Y, Zhou Y, Li G, Wang K, Bai P. Effective reduction of sintering temperature and breakage ratio for a low-cost ceramic proppant by feldspar addition. Int J Appl Ceram Technol 2018;15:191–6. https://doi.org/10.1111/ijac.12774.
[17] Deng ZY, Fukasawa T, Ando M, Zhang GJ, Ohji T. Microstructure and Mechanical Properties of Porous Alumina Ceramics Fabricated by the Decomposition of Aluminum Hydroxide. J Am Ceram Soc 2001;84:2638–44. https://doi.org/10.1111/j.1151-2916.2001.tb01065.x.
[18] Tian Z, Yang Y, Wang Y, Wu H, Liu W, Wu S. Fabrication and properties of a high porosity h-BN–SiO2 ceramics fabricated by stereolithography-based 3D printing. Mater Lett 2019;236:144–7. https://doi.org/10.1016/j.matlet.2018.10.058.
[19] Ramakrishna C, Thenepalli T, Huh JH, Ahn JW. Preparation of needle like aragonite precipitated calcium carbonate (PCC) from dolomite by carbonation method. J Korean Ceram Soc 2016;53:7–12. https://doi.org/10.4191/kcers.2016.53.1.7.
[20] Wu J, Li Z, Huang Y, Li F, Yang Q. Fabrication and characterization of low temperature co-fired cordierite glass-ceramics from potassium feldspar. J Alloys Compd 2014;583:248–53. https://doi.org/10.1016/j.jallcom.2013.08.187.
[21] She JH, Ohji T. Fabrication and characterization of highly porous mullite ceramics. Mater Chem Phys 2003;80:610–4. https://doi.org/10.1016/S0254-0584(03)00080-4.

Prapatsorn Prathungthai completed Ph.D from Suranaree University of Technology and working as a Lecturer in Department of Ceramics Design, Faculty of Architecture and Design, King Mongkut's University of Technology North Bangkok, Thailand.
Email: prapatsorn.p@archd.kmutnb.ac.th.